

Static disorder and structural correlations in the low temperature phase of lithium imide

Giacomo Miceli,^{1,2} Michele Ceriotti,² Marco Bernasconi,¹ and Michele Parrinello²

¹*Dept. of Materials Science, Università di Milano-Bicocca, via R. Cozzi 53, I-20125 Milano, Italy*

²*Computational Science, DCHAB, ETH Zurich, USI Campus, via G. Buffi 13, CH-6900 Lugano, Switzerland*

Based on *ab-initio* molecular dynamics simulations, we investigate the low temperature crystal structure of Li_2NH which in spite of its great interest as H-storage material is still matter of debate. The dynamical simulations reveal a precise correlation in the fractional occupation of Li sites which leads average atomic positions in excellent agreement with diffraction data and solves inconsistencies of previous proposals.

Lithium amide (LiNH_2) and imide (Li_2NH) have been extensively studied in recent years as promising materials for hydrogen storage[1–5]. Hydrogen release occurs in the mixture LiNH_2/LiH via a reversible solid state decomposition reaction into lithium imide and molecular hydrogen, $\text{LiNH}_2 + \text{LiH} \rightarrow \text{Li}_2\text{NH} + \text{H}_2$. The typical operating temperature for this system is around 280 °C, which is probably too high for on-board applications. Nevertheless, the amide/imide system is under deep scrutiny since it represents a prototypical, relatively simple system, which could shed light on the mechanisms of reversible H-release in the more complex, and technologically more promising, reactive hydrides made of mixtures of amide, borohidrides and/or alanates (e.g. $\text{LiNH}_2/\text{LiBH}_4$ or $\text{LiNH}_2/\text{NaAlH}_4$)[4, 5]. The search for better performing materials in this class would greatly benefit from a microscopic knowledge of the decomposition mechanism which requires in turn a detailed description of the crystalline phases involved. For several complex hydrides the structure of the phases undergoing the dehydrogenation/rehydrogenation process is still not fully resolved. This is the case for instance of the most studied sodium alanate (NaAlH_4) for which Raman spectroscopic data[6] and *ab-initio* simulations[7] very recently suggested the existence of a new high temperature phase which is expected to mediate the decomposition reaction in place of the low temperature α -phase considered so far. The structure of Li_2NH as well is still a matter of debate. Structural refinement from neutron and x-rays diffraction data reveals a structure of Li_2NH with fractional occupation. In spite of a substantial amount of experimental and theoretical investigation, the problem of the actual local structure which yields this long-range disorder is still unsettled. Based on *ab-initio* simulations, we have identified a model for the local structure of the low-temperature phase of lithium imide (Li_2NH) which solves inconsistencies of previous proposals and fully agree with experimental data available.

Differential thermal analysis and NMR measurements[8, 9] in the late 60's revealed a reversible phase transition at 356 K between an unknown low temperature (LT) structure and a high temperature antifluorite phase of Li_2NH . Structure refinement

from x-ray and neutron diffraction measurements on deuterated imide (Li_2ND) have been published only very recently[10]. The high temperature phase yields a diffraction pattern consistent with an anti-fluorite structure, in which hydrogen atoms occupy the 192l positions of the $Fm\bar{3}m$ space group. At low temperature (100-300 K) the diffraction data were best fitted by a cubic crystal with $Fd\bar{3}m$ space group. The LT crystal was described as a superstructure of the antifluorite phase in which one out of 8 Li atoms is displaced to an interstitial site giving rise to Li vacancies arranged in an ordered manner and tetrahedrally coordinated to four NH groups (Fig. 1(a)). The structure is stabilized by electrostatic interaction of $\text{H}^{\delta+}$ pointing towards the Li^+ vacancy which is formally a negatively charged site. Similar tetrahedral arrangements of four NH groups are present also in other imides, such as $\text{Li}_2\text{Mg}(\text{NH})_2$ [11]. In

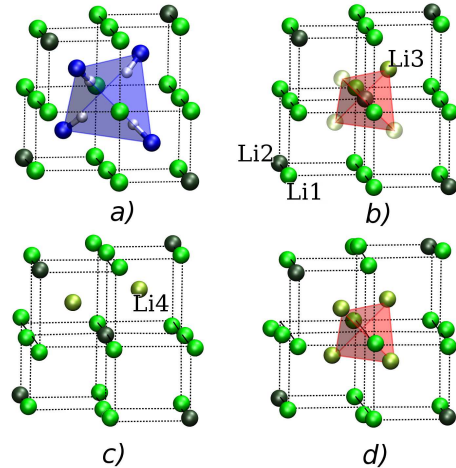


Figure 1. (a) Tetrahedral arrangement of NH groups around a Li^+ vacancy in the LT phase of Li_2NH . (b) Li ions are distributed on the three sites independent by symmetry labeled in panel. The interstitial Li3 sites have fractional occupation. Sites which are left empty in the *Ima2* model of Ref. [12] are shown as transparent spheres. (c) Occupied Li4 octahedral sites obtained upon relaxation of the *Ima2* model. (d) Our proposed correlation in the occupation of Li3 and Li2 sites leads to a tetrahedral cluster of four interstitial ions at Li3 sites around a vacancy at Li2 site.

the LT phase, H and N atoms occupy $32e$ sites. Li atoms are distributed over three different sites (Fig. 1(c)): $48f$ (Li1), $8a$ (Li2) and $32e$ (Li3). The Li3 site corresponds to a displacement along $\langle 111 \rangle$ directions from the octahedral position Li4 (sites $16d$ of the $Fd\bar{3}m$ space group, Fig. 1(c)). According to the Rietveld refinement, the latter has a fractional occupation of about $1/3$ at low temperatures, which only at room temperature gets closer to the value required by stoichiometry ($1/4$).

Diffraction data, however, do not provide information on correlations among the occupation of sites $32e$ which are mandatory to get full insight on the structural and dynamical properties of the system. To this aim, an attempt was made by Herbst and Hector to model the $Fd\bar{3}m$ crystal by fully occupying selected $32e$ sites [10, 12, 13]. In the structure proposed, a single Li^+ ion is present around each Li2 site, resulting in a $Ima2$ symmetry (Fig. 1(b)). The distance between Li2 and Li3 sites is, however, very small (1.53 \AA) and upon geometry optimization performed by *ab-initio* calculations[12], Li interstitials are displaced from Li3 sites into octahedral Li4 positions (sites $16d$ of the $Fd\bar{3}m$ space group) with a longer Li4-Li2 distance of 2.3 \AA (Fig. 1(c)). The locally relaxed structure obtained by Hector and Herbst [12] has $Imma$ symmetry and will be referred to hereafter as the HH phase. The positions of Li interstitials at Li4 sites are, however, incompatible with Rietveld refinement. Moreover, the theoretical formation energy of this phase is too high when compared to experimental data. Thus, other structures have been proposed on the basis of theoretical calculations, with Li atoms arranged in an ordered manner and a slightly lower formation energy[14, 15]. However, their equilibrium lattice parameters are inconsistent with the space group symmetry inferred experimentally. On the other hand, the local instability of the ideal antiferroite structure of Li ions at low temperature was confirmed by *ab-initio* molecular dynamics simulations at 300 K which showed the spontaneous formation of Li Frenkel pairs[16] and strong distortions of the Li sublattice[17].

Based on *ab-initio* simulations, we propose a structure for the LT phase which solves the problems mentioned above by introducing vacancies on partially occupied Li2 sites with a precise correlation with the occupation of Li3 interstitial sites. The solution of the puzzle came from the analysis of *ab-initio* molecular dynamics trajectories.

We started our analysis by performing *ab-initio* molecular dynamics simulations on the HH structure. A $\sqrt{2} \times 1 \times \sqrt{2}$, 128-atoms supercell corresponding to two $Imma$ unit cells was used. We performed Born-Oppenheimer molecular dynamics simulations within Density Functional Theory (DFT) with gradient corrected exchange and correlation functional[18] as implemented in the CPMD [19] package. Ultrasoft[20] and Goedecker-type[21] pseudopotentials were used, respectively, for N and H atoms and for Li with three valence electrons.

Kohn-Sham orbitals were expanded in plane waves up to a kinetic-energy cutoff of 50 Ry . Brillouin Zone (BZ) integration was restricted to the Γ point only. A time step of 0.6 fs was used and a constant temperature of 300 K was enforced by an optimal-sampling generalized Langevin equation thermostat[22]. Equilibrium geometries of relevant structures emerged from the dynamical simulations were optimized with special k-points meshes and the Quantum-Espresso suite of programs [23]. Activation energies for diffusion processes discussed below were obtained by Nudged Elastic Band optimizations[24].

In the dynamical simulations, 15 ps long, we observed that constitutional vacancies coordinated by NH groups are very stable, the latter performing only small librations around their equilibrium position. Instead, Li interstitials occupying Li4 positions are very mobile and we observed several jumps between adjacent sites, taking place via an exchange mechanism with one of the Li1 atoms (cf. Fig. S1 in supplementary materials below). The activation energy for diffusion of interstitials turns out to be as low as 0.13 eV . Moreover, we verified that many different arrangements of interstitial atoms in Li4 sites have total energies within few meV. At finite temperature, we would thus expect a disordered arrangement of interstitial atoms in the Li4 sites, leading to a fractional occupation of $1/2$ and an overall $Fd\bar{3}m$ space group.

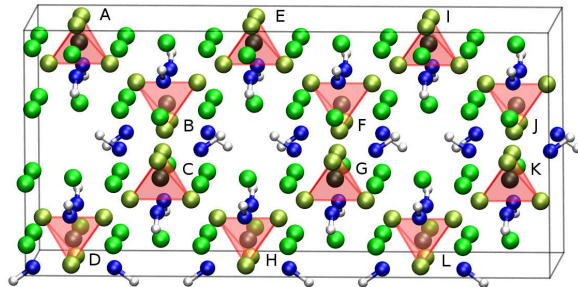


Figure 2. *a*) The 192 atoms supercell is shown ($3 \times 1 \times 1$ HH unit cells). The labeling indicates all possible sites where the four Li2 vacancy – Li3 interstitials clusters can be distributed inside the supercell. We found that the lowest-energy arrangements are *ACFL* (-30 meV/f.u. , see also Fig. S2 below) and *AEGK* (-29). Energies are given relative to the relaxed HH structure. Configurations where the tetrahedra are unevenly distributed such as *AEIC* (-17) or *ACEG* (4) are higher in energy, and those where nearest-neighbor sites are occupied simultaneously are even less stable.

However, the positions of Li4 still differ from those of Li3 obtained from Rietveld refinement. Moreover, the low diffusion barriers found would assign a superionic character to Li_2NH even at room temperature for which no experimental evidence has been provided so far.

The solution to these discrepancies came from a closer

inspection of the molecular dynamics trajectory, which revealed that as soon as three interstitial atoms happen to be all nearest neighbors to an occupied Li2 site, the latter atom is displaced from its position. A tetrahedral cluster is formed with a vacant Li2 site at its center (Fig. 1(d)). These clusters remain stable thereafter and prevent diffusion of Li interstitials. The interstitial Li now occupies the Li3 32e sites and a vacancy is introduced at site Li2 in such a way that the very short Li3-Li2 distance of the unrelaxed HH model is removed.

Having observed the propensity of Li atoms to form these rather stable tetrahedral structure, we propose a new stable structure in excellent agreement with diffraction data, as follows. At $T=0$ we expect that all the Li interstitials are involved in the formation of tetrahedral clusters. The smallest supercell compatible with this requirement and consistent with the stoichiometry is formed by $3 \times 1 \times 1$ HH unit cells (192 atoms). In such supercell there will be four vacancy-interstitials clusters, which can be distributed over twelve Li2 sites (see Figure 2). We considered all the possible arrangements of the vacancy-interstitials tetrahedra independent by symmetry excluding those where two first-neighbor Li3 sites are occupied.

Provided that the clusters are evenly distributed in the cell to balance the negatively-charged constitutional vacancies, the spread in the total energy of the different configurations is well within thermal energy at room temperature (see Fig. 2). We repeated our analysis on a larger $3 \times 1 \times 3$ supercell finding similar results. Such degeneracy allows for long-range disorder in the arrangement of tetrahedra, so that a diffraction pattern consistent with a higher-symmetry $Fd\bar{3}m$, with a fractional occupation of sites Li3 (1/3) and Li2 (2/3) is to be expected. These fractional occupations are compatible with the stoichiometry and solve the inconsistency in the model of Ref. [10].

By averaging over possible configurations of our 192-atoms supercell we obtained the symmetry-adapted average positions reported in Table I and the relative mean square displacements which would correspond to a static contribution to the Debye-Waller factor. The presence of clusters generates long-range distortions in the Li1 lattice and in the orientation of H atoms around a constitutional vacancy, resulting in a large mean square displacement from the average position for these species. The thermal Debye-Waller factors as a function of temperature have been computed from harmonic phonons (at the supercell Γ -point) and are given in Fig. S3 in supplementary materials below and at $T = 100$ K in Table I.

The agreement with the experimental positions from Rietveld refinement is excellent. The diffraction pattern of our proposed structure compares well with that deduced from the experimental positions and fractional occupation (Fig. S4 in supplementary materials below).

The formation enthalpy of the *ACFL* configuration (see Fig. 2) is lower (-30 meV f.u.⁻¹) than that of the

Site	x (exp. Ref [10])	U_{iso} static/thermal
N 32e f=1	0.2408 (0.2418)	0.34/0.50
D 32e f=1	0.2982 (0.2976)	1.58/2.00
Li1 48f f=1	0.3755 (0.3734)	2.18/0.93
Li2 8a f=2/3	–	0.25/0.87
Li3 32e f=1/3	0.0367 (0.0376)	0.22/0.91

Table I. Structural parameters of the best-fit $Fd\bar{3}m$ structure corresponding to the *ACFL* arrangement of tetrahedral clusters in a $3 \times 1 \times 1$ supercell (see Fig. 2). The Debye-Waller factor (10^{-2}\AA^2) is the sum of a contribution due to static disorder, and a thermal contribution calculated at $T = 100$ K for Li₂ND. The experimental data from Rietveld refinement of neutron diffraction patterns at 100 K from Ref. [10] are given in parentheses.

HH structure. Considering also zero-point energy and the harmonic contribution to the total free energy, our structure is still more stable than HH's (-18 meV f.u.⁻¹ at 298 K) and the structure proposed in Ref. [14] (-3 meV f.u.⁻¹). Our structure is slightly less stable (by 22 meV f.u.⁻¹) than that suggested in ref.[15] which however does not correspond to the experimental space group. However, uncertainties in the relative energies of the different phases are expected due to current approximations to the exchange and correlation functional as occurs for instance in other materials we have recently studied[25]. Moreover, entropic contributions due to disorder might compete with small enthalpy differences of ordered models and need to be taken into account before assigning the most stable phase at the DFT level. Because of all the above limitations, our aim was not to find the lowest possible ordered structure on the potential energy surface as pursued in Refs. [14, 15] but to refine a disordered structure which was a local minimum in DFT in such a way that is compatible with the experiments.

We verified the stability of the tetrahedral clusters by performing 20 ps of molecular dynamics at 300 K using the most stable arrangement *ACFL*. The vacancy-interstitials clusters do not break nor constitutional vacancies diffuse on the simulation time scale. The computed energy barrier to break a tetrahedral cluster by diffusion of a Li3 ion is indeed 0.5 eV, as obtained by NEB optimization, resulting in a low mobility of Li atoms in the LT phase (Li3 diffuses by an exchange mechanism similar to that of Li4, see Fig. S1 in supplementary materials below). The energy cost to break a cluster in the *ACFL* structure, via the reaction $4\text{Li3} \rightarrow \text{Li2} + 3\text{Li4}$ is $\Delta E=0.20$ eV. This energy depends on the final configuration of the interstitials, and on the number of clusters which are simultaneously broken. For instance, the difference in energy with the HH structure - with all the clusters broken - amounts to $\Delta E=0.36$ eV per cluster.

We can compute the change in configurational entropy due to breaking of tetrahedra and formation of these interstitial Li4 atoms, by assuming a perfectly ran-

dom distribution of tetrahedra and occupied Li4 interstitial sites (see supplementary materials below) which finally yields a concentration of broken tetrahedra of $x \sim \sqrt[3]{4/3} \exp[-\Delta E_0/3k_B T]$. This corresponds to a concentration at 300 K between $\sim 6\%$ and $\sim 0.5\%$, depending on the estimate taken for ΔE_0 . In spite of this large concentration of Li4 the diffusivity is still low because most of the percolating paths for Li4 interstitials are suppressed by the presence of Li3 atoms fixed in tetrahedra.

We speculate that the possible coexistence of partially occupied Li3 and Li4 sites might contribute to the change with temperature of the occupation of Li3 sites emerged from the Rietveld analysis [10]. We encourage new refinement of the diffraction data starting from our structural parameters in Table I, eventually allowing for a (small) partial occupation of sites Li4.

In summary, by combining *ab-initio* molecular dynamics and structural optimization, we have provided a full description of the structure of the LT phase of Li_2NH . Atomic positions coincide with those inferred from diffraction data but partial occupations of Li sites have a strong nearest neighbor correlation which solve the inconsistencies raised by previous proposals. This work represents an exemplary demonstration of how dynamical simulations can provide crucial insights to fully resolve the structure of systems with partial disorder, complementing experimental diffraction data.

We gratefully thank W. I. F. David for discussion and information.

-
- [1] P. Chen, Z. Xiong, J. Luo, J. Lin and K. L. Tan, *Nature* **420**, 302 (2002).
- [2] P. Chen, Z. Xiong, J. Luo, J. Lin, and K. L. Tan, *J. Phys. Chem. B* **107**, 10967 (2003).
- [3] D. H. Gregory, *J. Mat. Chem.* **18**, 1221 (2008).
- [4] P. Chen and M. Zhu, *Materials Today* **11**, 36 (2008).
- [5] S. Orimo, Y. Nakamori, J. F. Elise, A. Züttel, and C. M. Jensen, *Chem. Rev.* **107**, 4111 (2007).
- [6] H. Yukawa and *et al.*, *J. Alloys Compd.* **242**, 446 (2007).
- [7] B. C. Wood and N. Marzari, *Phys. Rev. Lett.* **103**, 185901 (2009).
- [8] R. A. Forman, *J. Chem. Phys.* **55**, 1987 (1971).
- [9] P.J. Haigh, R. A. Forman and R. C. Frish, *J. Chem. Phys.* **45**, 812 (1966).
- [10] M. P. Balogh, C. Y. Jones, J. F. Herbst, L. G. Hector Jr and M. Kundrat, *J. Alloys and Comp.* **420**, 326 (2006).
- [11] J. Rijssenbeek, Y. Gao, J. Hanson, Q. Huang, C. Jones, and B. Toby, *Journal of Alloys and Compounds* **454**, 233 (2008).
- [12] J. F. Herbst and L. G. Hector Jr, *Phys. Rev. B* **72**, 125120 (2005).
- [13] L. G. Hector Jr and J. F. Herbst, *J. Phys. Cond. Matt.* **20**, 064229 (2008).
- [14] B. Magyari-Köpe, V. Ozolins, and C. Wolverton, *Phys. Rev. B* **73**, 20101(R) (2006).
- [15] T. Mueller and G. Ceder, *Phys. Rev. B* **74**, 134104 (2006).
- [16] G. Miceli, C. Cucinotta, M. Bernasconi, and M. Parrinello, *J. Phys. Chem. C*, 302(2010).
- [17] G. A. Ludueña, M. Wegner, L. Bjalie, and D. Sebastiani, *Chem. Phys. Chem.* **11**, 2353 (2010).
- [18] J. P. Perdew, K. Burke, and M. Ernzerhof, *Phys. Rev. Lett.* **77**, 3865 (1996).
- [19] “CPMD,” <http://www.cpmc.org/>.
- [20] D. Vanderbilt, *Phys. Rev. B* **41**, 7892 (1990).
- [21] S. Goedecker, M. Teter, and J. Hutter, *Phys. Rev. B* **54**, 1703 (1996).
- [22] M. Ceriotti, G. Bussi, and M. Parrinello, *J. of Chem. Theory and Comput.* **6**, 1170 (2010).
- [23] P. Giannozzi *et al.*, “Quantum-espresso,” <http://www.quantum-espresso.org>, <http://www.pwscf.org>.
- [24] G. Henkelman, B. P. Uberuaga, and H. Jónsson, *J. Chem. Phys.* **113**, 9901 (2000).
- [25] G. Sosso, S. Caravati, C. Gatti, S. Assoni, and M. Bernasconi, *J. Phys. Cond. Matt.* **21**, 245401 (2009).

Supplementary materials

COMPUTATIONAL DETAILS

We started our analysis by performing ab-initio molecular dynamics simulations on the HH structure. A $\sqrt{2} \times 1 \times \sqrt{2}$, 128-atoms supercell corresponding to two *Imma* unit cells was used. We performed Born-Oppenheimer molecular dynamics simulations within Density Functional Theory with gradient corrected exchange and correlation functional[18] as implemented in the CPMD [19] package. Ultrasoft[20] and Goedecker-type[21] pseudopotentials were used, respectively, for N and H atoms and for Li with three valence electrons. Kohn-Sham orbitals were expanded in plane waves up to a kinetic-energy cutoff of 50 Ry. Brillouin Zone (BZ) integration was restricted to the Γ point only. A time step of 0.6 fs was used and a constant temperature of 300K was enforced by an optimal-sampling generalized Langevin equation thermostat[22]. Equilibrium geometries of relevant structures emerged from the dynamical simulations were optimized with special k-points meshes and the Quantum-Espresso suite of programs [23]. Activation energies for diffusion processes discussed below were obtained by Nudged Elastic Band optimizations [24].

MECHANISM OF DIFFUSION OF LI INTERSTITIALS

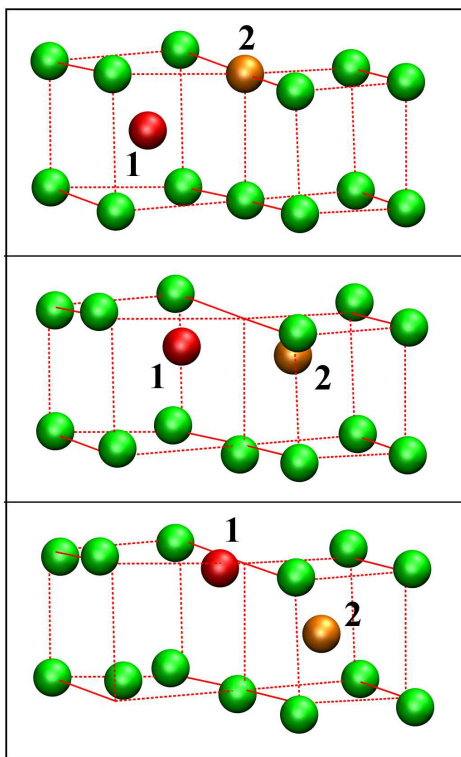


Figure S1. Diffusion exchange mechanism for Li interstitial. In the picture the initial, transition and final states are shown.

DEBYE-WALLER FACTOR

We calculated the Debye-Waller factor for each species as a function of the temperature from harmonic phonons. The mean square displacement as a function of the temperature in harmonic approximation is given by

$$\langle u_\alpha^2 \rangle = \frac{1}{N_\alpha} \sum_{m,i} \frac{\hbar}{\omega_m} \frac{|\mathbf{e}(m,i)|^2}{M_\alpha} \left[n_B \left(\frac{\hbar \omega_m}{k_B T} \right) + \frac{1}{2} \right] \quad (1)$$

where α runs over the atomic species, M_α is the mass of α th species, i runs over N_α atoms of species α , while ω_m and $\mathbf{e}(m,i)$ are the frequency and the eigenvector of the m th harmonic phonon.

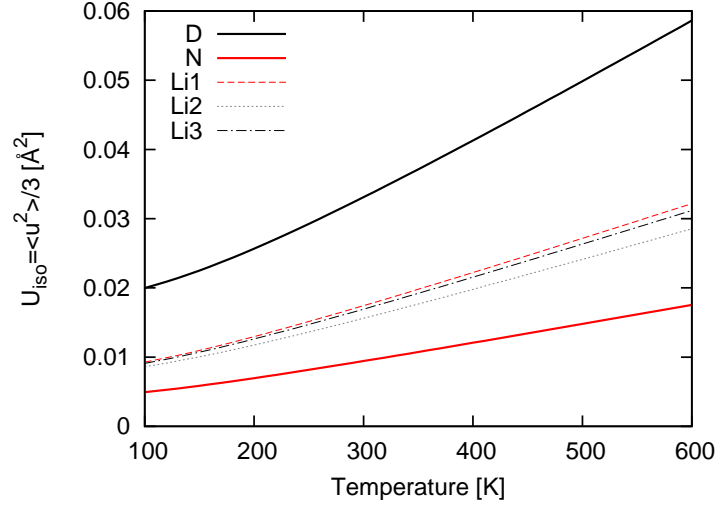


Figure S2. Debye-Waller factor, $U_{iso} = 1/3 \langle u_\alpha^2 \rangle$, for D, N, Li1, Li2, Li3 as a function of the temperature.

LI₂NH X-RAY DIFFRACTION PATTERN

We show in Fig. a comparison of the calculated x-ray diffraction pattern using both experimental [10] and our theoretical positions.

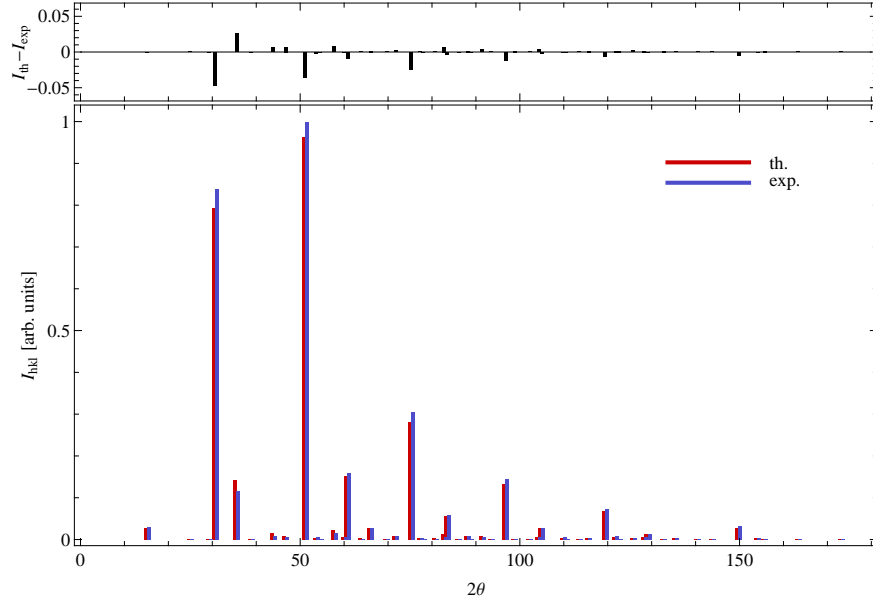


Figure S3. Bragg reflections intensities computed the average positions and occupations reported in Table 1, compared with those obtained using experimental values. No instrument-related corrections have been applied and the same Debye-Waller factor ($U_{iso} = 0.05 \text{ \AA}^2$) has been used for all atomic species.

CONFIGURATIONAL ENTROPY OF TETRAHEDRAL CLUSTERS

To compute the change in computational entropy due to the breaking of tetrahedra we considered that the number of tetrahedra N_T is related to the number of Li4 and Li2 sites by $N_{Li4} = 6N_T$ and $N_{Li2} = 3N_T$. The change in free energy due to the breaking of a fraction x of tetrahedra is given by

$$\frac{F}{N_T} = x\Delta E_0 - \frac{k_B T}{N_T} \left[\ln \left(\frac{3N_T}{N_T(1-x)} \right) - \ln \left(\frac{3N_T}{N_T} \right) \right] - \frac{k_B T}{N_T} \ln \left(\frac{N_T(2+4x)}{3xN_T} \right)$$

which yields an equilibrium concentration of

$$x \sim \sqrt[3]{4/3} \exp[-\Delta E_0/3k_B T].$$